World Academy of Science, Engineering and Technology
International Journal of Energy and Power Engineering
Vol:16, No:3, 2022

Practical Evaluation of High-Efficiency Si-Based Tandem Solar Cells

Sue-Yi Chen, Wei-Chun Hsu, Jon-Yiew Gan

***Abstract*—**Si-based double-junction tandem solar cells have become a popular research topic because of the advantages of low manufacturing cost and high energy conversion efficiency. However, there is no set of calculations to select the appropriate top cell materials. Therefore, this paper will propose a simple but practical selection method. First of all, we calculate the S-Q limit and explain the reasons for developing tandem solar cells. Secondly, we calculate the theoretical energy conversion efficiency of the double-junction tandem solar cells while combining the commercial monocrystalline Si and materials' practical efficiency to consider the actual situation. Finally, we conservatively conclude that if considering 75% performance of the theoretical energy conversion efficiency of the top cell, the suitable bandgap energy range will fall between 1.38 eV to 2.5 eV. Besides, we also briefly describe some improvements of several proper materials, CZTS, CdSe, Cu2O, ZnTe, and CdS, hoping that future research can select and manufacture high-efficiency Si-based tandem solar cells based on this paper successfully. Most importantly, our calculation method is not limited to silicon solely. If other materials' performances match or surpass silicon's ability in the future, researchers can also apply this set of deduction processes.

***Keywords*—**High-efficiency solar cells, material selection, Si-based double-junction solar cells, tandem solar cells, photovoltaics.

I. Introduction

SINCE the energy crisis and environmental contamination happened these days, significant studies have concentrated on developing renewable energy sternly to decrease non-renewable energy such as petroleum and natural gas. Specifically, among all kinds of renewable energy, solar cells that can convert solar energy into electrical energy are the subjects many people keep researching to create a promising future with sustainable energy and low environmental pollution. Also, to boost the competitiveness of the photovoltaic industry, lowering the Levelized Cost of Electricity (LCOE), is a critical indicator. Despite the high fabrication cost, if we successfully increase solar cells' energy conversion efficiency, people can reduce LCOE dramatically. Thus, to increase energy conversion efficiency, η, scientists are committed to research various methods and suitable materials to approach or exceed the S-Q limit, which was calculated by Shockley and Queisser [1].

One of the effective technologies is to build a tandem solar cell. By utilizing different bandgap widths, we can increase the absorption ratio of the solar spectrum, therefore achieving high energy conversion efficiency. For example, the energy conversion efficiency of a GaInP/GaAs/Si triple-junction tandem solar cell based on crystalline silicon can reach 35.9% [2]. Another triple-junction tandem solar cell, InGaP/GaAs/InGaAs, can also approach its energy conversion efficiency as high as 37.9% [2]. Therefore, we can realize that why tandem solar cells have tremendous potential for further development.

Generally speaking, there are two schemes of tandem solar cells. One is the design of a splitting spectrum; the other is based on stacking cells [3]. The first one utilizes several filters to separate different wavelengths of the solar spectrum. The benefit of such a structure is that every cell can perform independently that the current output of every cell will not influence others. Thus, theoretically, each cell's efficiency can reach close to the S-Q limit. However, due to the complex light path design, it is not easy to fabricate. The other approach exploits stacking materials as bottom cells with narrower bandgap width than the top ones through the whole solar cells, automatically splitting the solar spectrum to lower fabrication costs. Still, we can see from the research that though cell-stacking tandem solar cells can enhance energy conversion efficiency, with the increasing number of stacking cells, the improvement of efficiency would reduce [4]. Thus, under consideration to boost solar cells' efficiency while minimizing fabrication cost, this paper will focus specifically on cell-stacking double-junction tandem solar cells.

A typical cell-stacking double-junction tandem solar cell mainly uses materials with wide bandgap as the top cells to absorb short-wavelength sunlight. In contrast, materials with narrow bandgap are used as the bottom cells to absorb long-wavelength sunlight. Monocrystalline silicon (c-Si) is the one that occupies the current photovoltaic industry with low manufacturing cost, high energy conversion efficiency, and high stability. In addition, research had found that silicon is an ideal material for the bottom cell [5]. Still, when selecting appropriate materials for the top cells in Si-based tandem solar cells, researchers can only choose several possible materials based on theoretical energy conversion efficiency [6]. In a practical situation, these materials selected may not exert ideal effects. Thus, we exploit simple but effective equations to deduce how to choose suitable materials, in an actual circumstance, for the top cells of Si-based tandem solar cells according to bandgap width and making the overall energy conversion efficiency exceed 30%.

First, we briefly derive the S-Q limit and use it as a theoretical basis to confirm Si single-junction solar cell's ideal energy conversion efficiency. Secondly, the theoretical energy conversion efficiency of all kinds of tandem solar cells,

S.Y. Chen, W.C. Hsu, and J.Y. Gan are with the Department of Materials Science and Engineering, National Tsing Hua University, Hsinchu 300044, Taiwan R.O.C. (e-mail: sychenf@icloud.com, twjason88@gmail.com, jygan@mx.nthu.edu.tw).

including Si-based tandem solar cells, will be calculated. Last but not least, we will consider the practical situation and select materials from suitable bandgap energy as the top cells of Si-based tandem solar cells while discussing some improvements.

II. Calculations

A. Shockley-Queisser Limit

When calculating the energy conversion efficiency of single-junction solar cells, we first assume that all photons with energy more significant than the bandgap energy of materials are all absorbed. Therefore, we can obtain the maximum short-circuit current density:

$$J_{sc,max} = q\int_0^{\lambda(E_g)} \Phi(\lambda)d\lambda \quad (1)$$

where $\Phi(\lambda)$ is the photon flux under the AM1.5G spectrum [38], and q is the basic charge.

The open-circuit voltage, V_{oc}, is the maximum output voltage of a solar cell. For an ideal solar cell, we can describe its photoelectric curve:

$$J = J_{sc} - J_0\left[\exp\left(\frac{qV}{k_BT}\right) - 1\right] \approx J_{sc} - J_0\exp\left(\frac{qV}{k_BT}\right) \quad (2)$$

where V is the magnitude of the bias voltage, and k_B is the Boltzmann constant. When the current density $J = 0$, we have $V = V_{oc}$. Then we can express V_{oc} as:

$$V_{oc} = \frac{k_BT}{q}\ln\left(\frac{J_{sc}}{J_0} + 1\right) \quad (3)$$

where J_0 is the saturation current density. To calculate the limit value of J_0, we assume that a solar cell has a radiation behavior similar to that of a black body [1], which we call $J_{0,bb}$, or luminous flux of a black background body. The calculation method of $J_{0,bb}$ can be derived from the concept of quantum physics, and the integral formula is expanded through Taylor expansion to obtain an equation related to the bandgap energy E_g [7]:

$$J_{0,bb} = \frac{1}{2}\frac{(k_BT)^3}{\pi^2\hbar^3c^2}\left[\left(\frac{E_g}{k_BT}\right)^2 + 2\left(\frac{E_g}{k_BT}\right) + 2\right]\exp\left(-\frac{E_g}{k_BT}\right) \quad (4)$$

The fill factor, FF, is defined as the ratio of the maximum output power, P_{max}, of a solar cell to the product of the short-circuit current density, J_{sc}, and the open-circuit voltage, V_{oc}. *Green* also proposed an empirical formula of the fill factor expressed in the open-circuit voltage, V_{oc} [8]:

$$FF = \frac{P_{max}}{J_{sc}V_{oc}} = \frac{v_{oc} - \ln[v_{oc} + 0.72]}{v_{oc} + 1} \quad (5)$$

where $v_{oc} = (qV_{oc}/k_BT)$.

Finally, we can calculate the energy conversion efficiency of a solar cell [9]:

$$\eta(\%) = \frac{P_{max}}{P_{in,AM1.5G}} = \frac{J_{sc}V_{oc}FF}{P_{in,AM1.5G}} \times 100\% \quad (6)$$

where $P_{in,AM1.5G} = 1kW/m^2$ by integrating the AM1.5G spectrum [38]. According to (6), we can draw the theoretical energy conversion efficiency corresponding to different bandgap energy under the AM1.5G spectrum, as shown in Fig. 1.

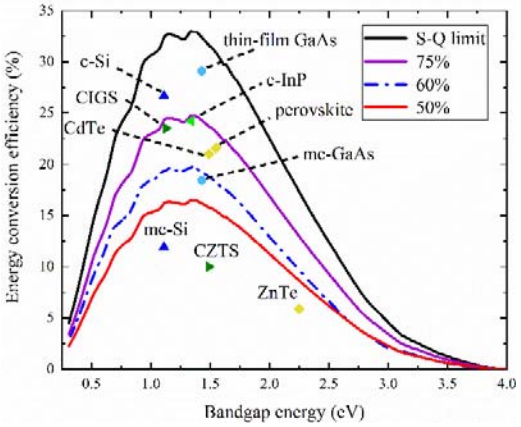

Fig. 1 Theoretical energy conversion efficiency limit for different bandgap widths. Only c-Si and GaAs can achieve close to the limit, with others merely laying under 75% of the theoretical value [2], [25]

As seen in Fig. 1, we can find out that the curve does not show as smooth as the one calculated by Shockley and Queisser [1] because the sunlight is affected by atmospheric absorption. Furthermore, we can notice that the value of the curve as a whole is bigger than the one expressed by Singh and Ravindra in 2012 [9] since the J_0 they had calculated was taken into account the collection efficiency of carriers in the solar cells. Nevertheless, when calculating the theoretical solar cell's efficiency, the mobility of carriers should be assumed to approach infinity, which means that the carrier collection efficiency is 100% [1]. Thus, the result we calculated will be much closer to the theoretical value. Also, according to Fig. 1, we can obtain the highest energy conversion efficiency, 33%, falling at the position where the bandgap energy equals 1.34 eV. In comparison, the highest energy conversion efficiency calculated by Rühle in 2016 is 33.7%, with the bandgap energy equals 1.34 eV [10]. Therefore, we consider that his value is close to our result, except with a slight discordance caused by the different settings of the solar cell's temperature. Rühle [10] assumed the cell's temperature to be 298 K, while we consider the temperature is 300 K. Furthermore, it can be seen from Fig. 1 that silicon (E_g = 1.11 eV), most commonly used material in the photovoltaic industry, corresponds to the ideal energy conversion efficiency of 32.35%. In addition, in the figure, we also draw the efficiency boundary curves of materials used in solar cells (η =50%, 75% of η_ideal) [11], and the reference efficiency used while selecting materials in the last part of the content (η = 60% of η_ideal). For all the data points in Fig. 1, only c-Si and GaAs, III-V compound semiconductors, are the closest materials to the S-Q limit. In contrast, others including CIGS, perovskite, CZTS, etc., are still far from the theoretical limit. Most of them lie between 50% and 75% of the theoretical efficiency.

B. The Theoretical Efficiency of Tandem Cells

We use a simple formula to calculate the theoretical energy conversion efficiency of constrained double-junction tandem solar cells and further explore Si-based solar cells in the actual situation.

Under the *S-Q limit* assumption, when sunlight enters a solar cell, photons in the short-wavelength range can be absorbed entirely by the top cell to generate photocurrent at the top, which is called $J_{sc,top}$, and the calculation method remains the same as (1). On the other hand, the photons in the long-wavelength range are absorbed by the bottom cell to generate photocurrent at the bottom, which is called $J_{sc,bot}$. It should be noted that we cannot directly calculate the photocurrent generated by the bottom cell via (1) because the photon energy absorbed by the bottom cell is leftover which the top cell cannot absorb; therefore, (1) must be revised slightly as:

$$J_{sc,bot} = q\int_{\lambda(E_{g,top})}^{\lambda(E_{g,bot})} \Phi(\lambda)d\lambda \tag{7}$$

Most importantly, we neglect photons generated from top and bottom cells when calculating $J_{sc,top}$ and $J_{sc,bot}$ because the photocurrent generated by such a mechanism is ignorable [4]. Besides, due to constrained output mode, the overall short-circuit current of tandem solar cells will depend on the cells with insufficient output current. Accordingly, the smaller one of $J_{sc,top}$ or $J_{sc,bot}$ will become the final output current, J_{sc}, namely $\min(J_{sc,top}, J_{sc,bot})$ [12].

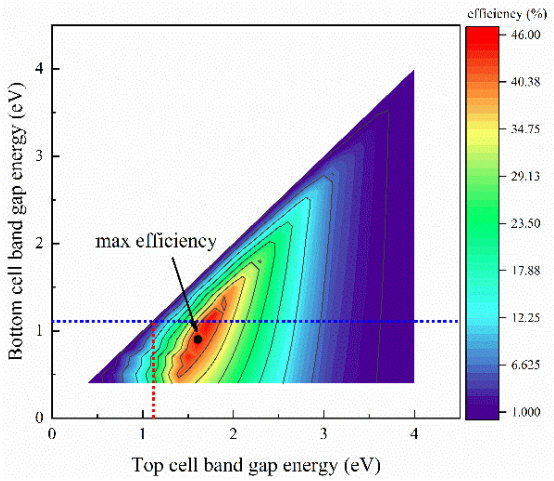

Fig. 2 A contour map of theoretical energy conversion efficiency of double-junction tandem solar cells. The maximum efficiency (η = 45.84%) occurs when the top cell acquires 1.6 eV bandgap energy, and the bottom cell obtains 0.9 eV, respectively

The open-circuit voltage, V_{oc}, of the top and bottom cells can each be expressed as:

$$V_{oc,top} = \frac{k_B T}{q}\ln\left(\frac{J_{sc}}{J_{0,bb-top}} + 1\right) \tag{8}$$

$$V_{oc,bot} = \frac{k_B T}{q}\ln\left(\frac{J_{sc}}{J_{0,bb-bot}} + 1\right) \tag{9}$$

Moreover, since the output mode is constrained, the total open-circuit voltage of the solar cell can be expressed as [12]:

$$V_{oc,overall} = V_{oc,top} + V_{oc,bot} \tag{10}$$

Besides, because this is the calculation of ideal tandem solar cells, the recombination mechanism of both the top and bottom cells is still dominated by the light-emitting recombination mechanism. Thus, the $J_{0,bb-top}$ and $J_{0,bb-bot}$ in (8) and (9) can be directly calculated by (4).

As for the fill factor, the difference with (5) is that we use the ideal fill factor for calculation:

$$FF_{ideal} = \frac{(qV_{oc,overall}/k_B T) - \ln[(qV_{oc,overall}/k_B T)+1]}{(qV_{oc,overall}/k_B T)+1} \tag{11}$$

Finally, the energy conversion efficiency of constrained tandem solar cells can be expressed as [15]:

$$\eta(\%) = \frac{P_{out,overall}}{P_{in,AM1.5G}} = \frac{J_{sc}V_{oc,overall}FF_{ideal}}{P_{in,AM1.5G}} \times 100\% \tag{12}$$

Through (7)-(12), we could use the bandgap width of the top cells as a horizontal axis and that of the bottom cells as a vertical axis to draw an efficiency contour map of constrained double-junction tandem solar cells, as shown in Fig. 2. It should be noted that the purpose of this calculation is to obtain an approximate outline of the theoretical efficiency through the use of simple formulas and derivations. Therefore, we used 0.1 eV as a unit for the magnitude change in the bandgap width of both top and bottom cells for calculations.

We can see from Fig. 2 that the graph presents a triangular shape because of a basic assumption: the bandgap energy of the top cell must be greater than that of the bottom cell. Thus, when the bandgap energy of the bottom cell is more significant than that of the top cell, the pattern does not exist. Moreover, when the top and bottom cells both have the same bandgap width, the top cell will absorb all the photons that the bottom cell can absorb, which will cause the photocurrent of the bottom cell to become zero. Accordingly, due to the constrained output mode, the overall short-circuit current will become zero, leading to zero efficiency. In addition, when the bandgap energy of the top cell is 1.6 eV, and that of the bottom cell is 0.9 eV, the solar cell will obtain the highest theoretical energy conversion efficiency, 45.84%. This data is very close to the result calculated by Bremner et al. in 2008. Similarly, they found that when the bandgap energy of the top cell is 1.6 4 eV, and that of the bottom cell is 0.9 eV, the double-junction tandem solar cell has the highest theoretical efficiency of 45.71% [13]. However, our result is slightly different from the result presented in PVCDROM. The highest efficiency of the double-junction tandem solar cell calculated by PVCDROM occurs when the bandgap energy of the top cell is 1.63 eV, and that of the bottom cell is 0.96 eV, which has 47% [14]. We believe that this difference can be eliminated by reducing the magnitude change in bandgap width to 0.01 eV.

C.Si-Based Double-Junction Tandem Solar Cells-Constrained Si-Based Tandem Solar Cells

After calculating the theoretical energy conversion efficiency of tandem solar cells, we discuss the particular efficiency when silicon (E_g = 1.11 eV) becomes the top and bottom cells, respectively. We, therefore, extract the data from the red and blue lines marked in Fig. 2 to draw Fig. 3.

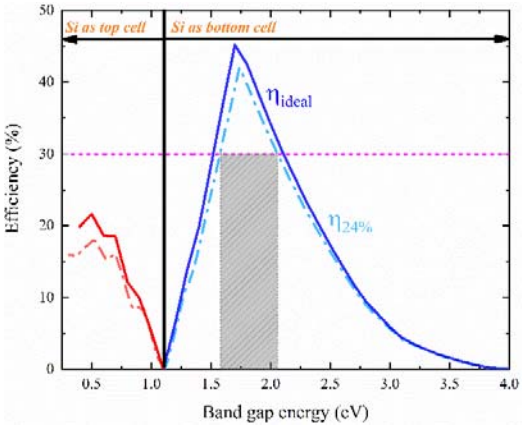

Fig. 3 The relationship between the energy conversion efficiency of Si-based tandem solar cells and the bandgap energy of the other stacking cells. The solid line represents the ideal situation, while the dotted line represents the circumstance that considers c-Si 24% but with the other stacking cells remaining ideal. The gray area shows the bandgap energy range for suitable material selection (1.57~2.05 eV), where c-Si 24% acts as the bottom cell while assuming the top cell material performs theoretically

In Fig. 3, the overall efficiency will drop to zero when both the top and bottom cells are Si, leading to no light absorption in the bottom cell. In addition, when silicon acts as the top cell, too many long-wavelength photons will not be absorbed by the bottom cell to generate enough photocurrent, making the energy conversion efficiency low. However, when silicon acts as the bottom cell, such loss is much less. Thus, we can find that the energy conversion efficiency curve has the highest point. So, the highest efficiency value happens when the top and bottom cells' currents match appropriately. We can also see from Fig. 3 that the theoretical energy conversion efficiency of a tandem solar cell with silicon as the bottom cell can reach as high as 45% when the bandgap energy of the top cell is 1.7 eV. Such high efficiency is almost 1.5 times the theoretical energy conversion efficiency of a silicon single-junction solar cell, championing the promising potential for tandem solar cells. However, there is always a gap between theoretical efficiency and the actual situation. Therefore, to discuss suitable choices for the top cell materials in Si-based tandem solar cells in practical applications, we set the efficiency of silicon cells to the current commercial efficiency c-Si 24% [2]. After calculation, we can get the dotted line in Fig. 3. To find the ideal corresponding top cell materials, we used the energy conversion efficiency, 30%, as a benchmark. The reason for choosing 30% is that it is the most apparent difference of performance between tandem cells and single-junction silicon cells. Specifically, not many suitable materials can make the energy conversion efficiency reach 30% in developing single-junction cells. Currently, GaAs thin-film solar cell has the highest value, 29.1% [2]. Therefore, if there is an ideal top cell material, which can make the overall tandem solar cells' efficiency exceed 30%, we will consider such material to have a promising potential.

We can find out that when considering the practical efficiency of c-Si, the theoretical bandgap energy range for selecting top cell materials lies between 1.57 eV and 2.05 eV. However, the bandgap range is relatively small. Furthermore, if we consider the actual situation of the top cells, the range will reduce further. Assuming that we expect to have more choices, we need to ease the change of energy conversion efficiency versus bandgap energy in Fig. 3 while increasing the overall efficiency. Accordingly, we decide to use unconstrained tandem solar cells to repeat our calculations.

D.Si-Based Double-Junction Tandem Solar Cells-Unconstrained Si-Based Tandem Solar Cells

The energy conversion efficiency calculation for the unconstrained tandem solar cells is quite similar to that of the constrained ones. The current and voltage are the same as (7)-(9). The difference is that due to the unconstrained output mode, the output current of the top and bottom cells does not affect each other; thus, there is no need for current matching. Besides, because cells are not connected in series, we cannot directly add the voltage of the top and bottom cells together to get the total output voltage. Instead, we have to calculate the overall efficiency by separately calculating the energy conversion efficiency of the top and bottom cells via (12), then adding them together [15]. We can rewrite (12) as:

$$\eta(\%) = \frac{P_{out,top}+P_{out,bot}}{P_{in,AM1.5G}} \times 100\% \quad (13)$$

Subsequently, we can draw Fig. 4 based on Fig. 3. The solid gray line in Fig. 4 is the theoretical energy conversion efficiency of the overall solar cells obtained after considering that silicon and other materials are ideal. We can find that the solid gray line is much gentler than the solid blue line in Fig. 3.

In theory, all materials in the bandgap range 1.12 eV to 4 eV can make the efficiency of Si-based tandem solar cells exceed 30%, significantly increasing the opportunity of material selection. In addition, the highest theoretical energy conversion efficiency can reach 44.3%, which shows the capacity of the unconstrained output mode for developing Si-based tandem solar cells in the future.

To get closer to the actual situation, we again consider the commercial c-Si ($\eta = 24\%$) as mentioned above. Besides, we use 100%, 75%, and 60% of the ideal energy conversion efficiency of the other stacking cells as principles to draw the overall efficiency individually shown as blue, red, and green solid lines. The dotted lines are the energy conversion efficiency of the other stacking cells alone.

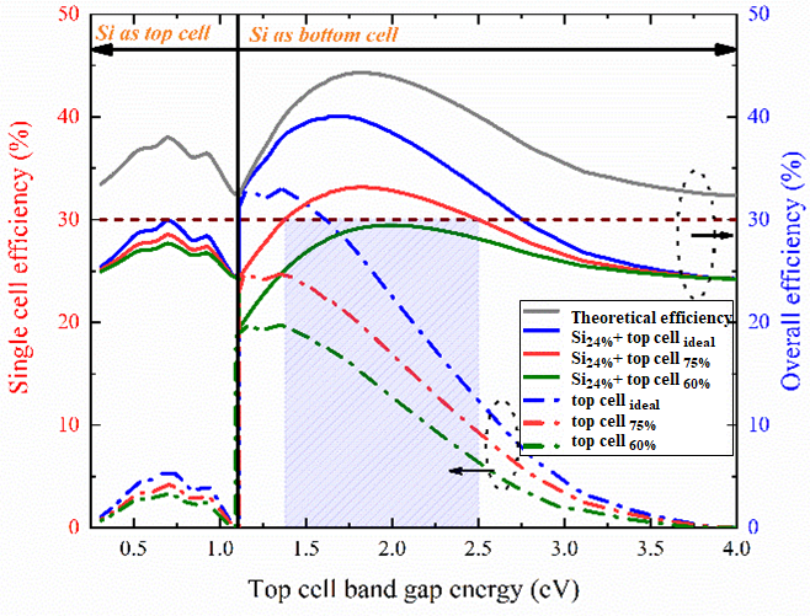

Fig. 4 The relationship between the energy conversion efficiency of unconstrained Si-based tandem solar cells and the bandgap energy of the other stacking cells. The solid gray line represents the overall theoretical efficiency. Others colored solid lines show the overall efficiency when considering commercial c-Si with 100%, 75%, and 60% of the ideal efficiency of the other stacking cells, respectively. The dotted lines are the energy conversion efficiency of the different stacking cells alone. The purple area offers the suitable range of bandgap energy of the top cells that can make high-efficiency tandem solar cells

III. Results and Discussion

A. Bandgap Range Determination

Observing the solid blue line in Fig. 4, we find that compared with the blue dashed line in Fig. 3, the efficiency curve of the overall tandem solar cell changes more slowly with the bandgap energy because of the different output mode. Besides, seeing from the red and green solid lines, the energy conversion efficiency is also lower than that in Fig. 3 because we reduced the efficiency performance of the top cells. However, the same thing is that when using silicon as the top cell, the energy conversion efficiency of the overall solar cell is relatively low. Therefore, we can also view silicon as the bottom cell as usual.

We assume that the efficiency of the bottom cell, c-Si, is set to 24%. In that case, we can notice that when the ideal top cell acquires bandgap energy in the range of 1.12 eV to 2.75 eV, the efficiency of the overall solar cell can reach more than 30%. Moreover, when the bandgap energy of the top cell is 1.63 eV, there will be the highest overall efficiency, 40.08%, as shown by the solid blue line (Fig. 4). Unfortunately, there is not any material that can truly achieve 100% of theoretical efficiency. Therefore, we revised the energy conversion efficiency of the top cell, as shown by the red and green solid lines. As the efficiency of the top cell decreases, the bandgap range of materials that can be selected as the top cell will become smaller, and the energy conversion efficiency of the overall solar cell will also decrease. Moreover, when the energy conversion efficiency of the top cell becomes lower than 60% of the theoretical efficiency, the overall efficiency will always be lower than 30%. Thus, we conservatively conclude that if the solar cell is to achieve high-efficiency performance ($\eta \geq 30\%$), the energy conversion efficiency of the top cell must be greater than 75% of the theoretical value. Finally, we will discuss some suitable materials based on 75% of the theoretical energy conversion efficiency.

TABLE I
Correspondence Table of Materials and Bandgap Energy [31]-[37]

E_g(eV)	1,43	1,49	1.49~1.63	1,6	1,7	1.7~1.8	1,74	1,8
Material	GaAs	CdTe	CZTS	AlSb	Sb_2S_3	a-Si:H	CdSe	MoS_2
E_g(eV)	2,1	2,16	2,17	2,2	2,25	2,26	2,42	2,45
Material	GaSe	AlAs	Cu_2O	SnS_2	ZnTe	GaP	CdS	AlP

From the solid red line in Fig. 4 and the purple area below it, we can notice that under the condition that the top cell has 75% of the theoretical efficiency, to achieve high efficiency of the overall tandem solar cell, its bandgap energy must fall between 1.38 eV and 2.5 eV. Table I lists some of the corresponding bandgap widths and types of semiconductor materials. To reach high efficiency, we also have to consider carrier mobility, direct bandgap, material dimensions, etc. Accordingly, we selected some possible materials from Table I that are colored in the blue area. However, the truth is that in addition to GaAs and CdTe, which can exceed 75% and 65% of the theoretical energy conversion efficiency, respectively [2], the current efficiency performance of other materials is poor. Thus, we propose some improvements, hoping that researchers will find more suitable top cell materials soon.

B. Material Improvements

CdSe: The bandgap energy of CdSe is very close to 1.8 eV, which corresponds to the highest efficiency in the solid red line in Fig. 4. In addition, CdSe is a direct bandgap material and owns a high absorption coefficient in the visible wavelength

range [16], which should have considerable potential. However, since studies had proposed in 1982 to manufacture CdSe thin-film solar cells with an energy conversion efficiency of more than 6% [16], there has not been a significant improvement these days. Mahawela et al. mentioned in 2005 that the short-circuit current of a CIGS-based tandem solar cell with CdSe as the top cell was able to exceed 17 mA/cm^2, but with the open-circuit voltage obtained only 475 mV. They believed that the energy conversion efficiency could be further increased by improving the contact surface between materials [17]. In addition, Patel et al. found in 2019 that when treating CdSe film with $CdCl_2$, CdSe could acquire higher crystallinity, larger grain size, and flatter surface [18]. They concluded that this method could also effectively boost solar cells. Therefore, it is not doom to enhance the efficiency of CdSe solar cells in the future.

Cu_2O: This is one of the few studied P-type semiconductor materials with transition metal oxide and high hole mobility [19]. In the early days, the efficiency of solar cells made of ZnO/Cu_2O was only 0.88% [20]. Nevertheless, currently, through high-temperature oxidation of Cu substrate, high-quality Cu_2O is obtained. Besides, adding the number of stacking cells can also increase the energy conversion efficiency of Cu_2O tandem solar cells to 8.1% [21]. Still, stacking too many materials and undergoing high-temperature processes will increase the cost. Therefore, Zang proposed a new method in 2018, utilizing radiation oxidation to get Cu_2O crystals, followed by rapid quenching and annealing to obtain high-quality Cu_2O while enlarging the grain size. Finally, a ZnO/Cu_2O solar cell with an efficiency of 3.18% was acquired [22]. Although the efficiency was slightly insufficient for applications, it should be improved through additional surface treatment. Overall, Cu_2O is still a material with promising potential.

ZnTe: This is often used as the buffer layer for CdTe solar cells [23], but it is rarely used as single-junction solar cells. One of the main reasons is that P-type ZnTe is easier to make than N-type ZnTe. Tanaka et al. proposed in 2010 making N-type ZnTe by thermal diffusion of Al into P-type ZnTe in the same way as LEDs to construct ZnTe single-junction solar cell; however, its efficiency was only 0.78% [24]. They speculated that the reason for low efficiency was due to material defects caused by Al. Therefore, they believed that by improving the quality of Al diffusion layers, cell efficiency would be further promoted in the future. In addition, P-type ZnTe can also be made by Cr doping with laser pulse deposition [25]. Research has found that ZnTe doped with Cr had a higher absorption coefficient and thermal stability. Furthermore, after making into intermediate band solar cells (IBSC), the short-circuit current and open-circuit voltage would be enhanced, increasing the efficiency to 5.9% [25]. In other studies, cell efficiency can also be improved by adding a back-surface-field (BSF) layer. For instance, the BSF layer made of PbTe can reduce carrier recombination and increase carrier collection rate, increasing the simulated battery efficiency by 4.6% [26]. As mentioned above, these studies prove that ZnTe is another candidate for building high-efficiency solar cells.

CdS: From the research of Shitaya and Sato in 1968, we know that it is challenging to make P-type CdS with high conductivity [27]. Because the material structure is very similar, current research mainly applies CdS to CdS/CdTe or CdS/ZnTe tandem cells to increase its efficiency to 15.8% [28]. Alternatively, Cds can be used in the form of quantum dots in the GaAs-based solar cell with an energy conversion efficiency of 18.9%. [29]. In 2016, Deng et al. further proposed that using Cu to make P-type CdS would damage the optical properties of CdS. In addition, they also mentioned that when stacking P-type Cds made by Cu with CdTe, the fill factor and open-circuit voltage would decrease significantly [30]. Thus, to obtain high efficiency, one of the improved directions is to develop new ways to manufacture P-type CdS.

IV. Conclusion

We propose a series of deductions for selecting top cell materials for the silicon-based tandem solar cells. In the results, if the bottom cell is the commercial c-Si while the top cell material remains ideal, to achieve high efficiency, the bandgap energy of the top cell materials will lie between 1.12 eV and 2.75 eV. However, this range will reduce further in a practical situation. If we consider 75% of the theoretical energy conversion efficiency of the top cell, the suitable bandgap energy range will fall between 1.38 eV to 2.5 eV. If we choose less than 60% of the theoretical efficiency, the overall efficiency will always be less than 30%. Finally, based on 75% of the theoretical efficiency, we briefly discussed some improvement directions of cell materials, CZTS, CdSe, Cu_2O, ZnTe, and CdS within the specific bandgap range, including PN-type semiconductor process technology, material quality, and suitable element replacement. It is expected that these potential materials will be used in the future to achieve high-efficiency double-junction Si-based tandem solar cells. Of course, most importantly, this calculation is not merely limited to silicon. If other materials' performances can match or surpass silicon's ability in the future, researchers can also apply this deduction set.

References

[1] Shockley, W., Queisser, H.J., 1961. Detailed balance limit of efficiency of p-n junction solar cells. J. Appl. Phys. 32, 510–519. https://doi.org/10.1063/1.1736034

[2] Green, M., Dunlop, E., Hohl-Ebinger, J., Yoshita, M., Kopidakis, N., Hao, X., 2021. Solar cell efficiency tables (version 57). Prog. Photovoltaics Res. Appl. 29, 3–15. https://doi.org/10.1002/pip.3371

[3] Nelson, J., 2003. The Physics of Solar Cells, The Physics of Solar Cells. Published by Imperial College Press and Distributed by World Scientific Publishing CO. https://doi.org/ 10.1142/p276

[4] De Vos, A., 1980. Detailed balance limit of the efficiency of tandem solar cells. J. Phys. D. Appl. Phys. 13, 839–846. https://doi.org/10.1088/0022-3727/13/5/018

[5] Yamaguchi, M., Lee, K.H., Araki, K., Kojima, N., 2018. A review of recent progress in heterogeneous silicon tandem solar cells. J. Phys. D. Appl. Phys. https://doi.org/10.1088/1361-6463/aaaf08

[6] Lu, S., Chen, C., Tang, J., 2020. Possible top cells for next-generation Si-based tandem solar cells. Front. Optoelectron. https://doi.org/ 10.1007/s12200-020-1050-y

[7] Smestad, G., Ries, H., 1992. Luminescence and current-voltage characteristics of solar cells and optoelectronic devices. Sol. Energy Mater. Sol. Cells 25, 51–71. https://doi.org/10.1016/0927-

0248(92)90016-I
[8] Green, M.A., 1982. Operating Principles, Technology and System Applications Paperback. United States. https://doi.org/10.2172/1644255
[9] Singh, P., Ravindra, N.M., 2012. Temperature dependence of solar cell performance - An analysis. Sol. Energy Mater. Sol. Cells 101, 36–45. https://doi.org/10.1016/j.solmat.2012.02.019
[10] Rühle, S., 2016. Tabulated values of the Shockley-Queisser limit for single junction solar cells. Sol. Energy 130, 139–147. https://doi.org/10.1016/j.solener.2016.02.015
[11] Polman, A., Knight, M., Garnett, E.C., Ehrler, B., Sinke, W.C., 2016. Photovoltaic materials: Present efficiencies and future challenges. Science (80-.). https://doi.org/10.1126/science.aad4424
[12] Ehrler, B., Alarcón-Lladó, E., Tabernig, S.W., Veeken, T., Garnett, E.C., Polman, A., 2020. Photovoltaics reaching for the shockley-queisser limit. ACS Energy Lett. 5, 3029–3033. https://doi.org/10.1021/acsenergylett.0c01790
[13] Bremner, S.P., Levy, M.Y., Honsberg, C.B., 2008. Analysis of tandem solar cell efficiencies under AM1.5G spectrum using a rapid flux calculation method. Prog. Photovoltaics Res. Appl. 16, 225–233. https://doi.org/10.1002/pip.799
[14] S.G.Bowden, C.B.Honsberg, 2019. Tandem Cells | PVEducation (WWW Document) URL https://www.pveducation.org/pvcdrom/tandem-cells (accessed 9.1.21).
[15] Li, Z., Xiao, H., Wang, X., Wang, C., Deng, Q., Jing, L., Ding, J., Hou, X., 2013. Theoretical simulations of InGaN/Si mechanically stacked two-junction solar cell. Phys. B Condens. Matter 414, 110–114. https://doi.org/10.1016/j.physb.2013.01.026
[16] Rickus, E., 1982. Photovoltaic Behaviour of CdSe Thin Film Solar Cells, in: Commission of the European Communities, (Report) EUR. Springer, Dordrecht, pp. 831–883. https://doi.org/10.1007/ 978-94-009-7898-0_139
[17] Mahawela, P., Jeedigunta, S., Vakkalanka, S., Ferekides, C.S., Morel, D.L., 2005. Transparent high-performance CDSE thin-film solar cells, in: Thin Solid Films. Elsevier, pp. 466–470. https://doi.org/10.1016/j.tsf.2004.11.066
[18] Patel, S.L., Himanshu, Chander, S., Purohit, A., Kannan, M.D., Dhaka, M.S., 2019. Understanding the physical properties of CdCl2 treated thin CdSe films for solar cell applications. Opt. Mater. (Amst). 89, 42–47. https://doi.org/10.1016/j.optmat.2019.01.001
[19] Miyata, T., Tanaka, H., Sato, H., Minami, T., 2006. P-type semiconducting Cu2O-NiO thin films prepared by magnetron sputtering. J. Mater. Sci. 41, 5531–5537. https://doi.org/10.1007/s10853-006-0271-9
[20] Cui, J., Gibson, U.J., 2010. A simple two-step electrodeposition of Cu2O/ZnO Nanopillar solar cells. J. Phys. Chem. C 114, 6408–6412. https://doi.org/10.1021/jp1004314
[21] Minami, T., Nishi, Y., Miyata, T., 2016. Efficiency enhancement using a Zn1-xGex-O thin film as an n-type window layer in Cu2O-based heterojunction solar cells. Appl. Phys. Express 9, 052301. https://doi.org/10.7567/APEX.9.052301
[22] Zang, Z., 2018. Efficiency enhancement of ZnO/Cu2O solar cells with well oriented and micrometer grain sized Cu2O films. Appl. Phys. Lett. 112, 042106. https://doi.org/10.1063/1.5017002
[23] Wolden, C.A., Abbas, A., Li, J., Diercks, D.R., Meysing, D.M., Ohno, T.R., Beach, J.D., Barnes, T.M., Walls, J.M., 2016. The roles of ZnTe buffer layers on CdTe solar cell performance. Sol. Energy Mater. Sol. Cells 147, 203–210. https://doi.org/10.1016/j.solmat.2015.12.019
[24] Tanaka, T., Yu, K.M., Stone, P.R., Beeman, J.W., Dubon, O.D., Reichertz, L.A., Kao, V.M., Nishio, M., Walukiewicz, W., 2010. Demonstration of homojunction ZnTe solar cells. J. Appl. Phys. 108, 024502. https://doi.org/10.1063/1.3463421
[25] Lee, K.S., Oh, G., Chu, D., Pak, S.W., Kim, E.K., 2017. High power conversion efficiency of intermediate band photovoltaic solar cell based on Cr-doped ZnTe. Sol. Energy Mater. Sol. Cells 170, 27–32. https://doi.org/10.1016/j.solmat.2017.05.020
[26] Dey, Mrinmoy, Asha, I.A., Smita, Z.T., Dey, Maitry, Das, N.K., 2019. Highly efficient ZnTe solar cell with PbTe BSF, in: 2019 5th International Conference on Advances in Electrical Engineering, ICAEE 2019. Institute of Electrical and Electronics Engineers Inc., pp. 613–616. https://doi.org/10.1109/ICAEE48663.2019.8975498
[27] Shitaya, T., Sato, H., 1968. Single Crystal CdS Solar Cell. Jpn. J. Appl. Phys. 7, 1348–1353. https://doi.org/10.1143/jjap.7.1348
[28] Britt, J., Ferekides, C., 1993. Thin-film CdS/CdTe solar cell with 15.8% efficiency. Appl. Phys. Lett. 62, 2851–2852. https://doi.org/10.1063/1.109629
[29] Lin, C.-C., Chen, H.-C., Tsai, Y.L., Han, H.-V., Shih, H.-S., Chang, Y.-A., Kuo, H.-C., Yu, P., 2012. Highly efficient CdS-quantum-dot-sensitized GaAs solar cells. Opt. Express 20, A319. https://doi.org/10.1364/oe.20.00a319
[30] Deng, Y., Yang, J., Yang, R., Shen, K., Wang, Dezhao, Wang, Deliang, 2016. Cu-doped CdS and its application in CdTe thin film solar cell. AIP Adv. 6, 015203. https://doi.org/10.1063/1.4939817
[31] Arora, H., Erbe, A., 2021. Recent progress in contact, mobility, and encapsulation engineering of InSe and GaSe. InfoMat 3, 662–693. https://doi.org/10.1002/inf2.12160
[32] Burton, L.A., Whittles, T.J., Hesp, D., Linhart, W.M., Skelton, J.M., Hou, B., Webster, R.F., O'Dowd, G., Reece, C., Cherns, D., Fermin, D.J., Veal, T.D., Dhanak, V.R., Walsh, A., 2016. Electronic and optical properties of single crystal SnS2: an earth-abundant disulfide photocatalyst. J. Mater. Chem. A 4, 1312–1318. https://doi.org/10.1039/C5TA08214E
[33] DeAngelis, A.D., Kemp, K.C., Gaillard, N., Kim, K.S., 2016. Antimony(III) Sulfide Thin Films as a Photoanode Material in Photocatalytic Water Splitting. ACS Appl. Mater. Interfaces 8, 8445–8451. https://doi.org/10.1021/acsami.5b12178
[34] Kasap, S., Capper, P. (Eds.), 2007. Springer Handbook of Electronic and Photonic Materials, Springer Handbook of Electronic and Photonic Materials, Springer Handbooks. Springer International Publishing, Cham. https://doi.org/10.1007/978-0-387-29185-7
[35] Madelung, O., Rössler, U., Schulz, M. (Eds.), n.d. Cuprous oxide (Cu2O) band structure, band energies: Datasheet from Landolt-Börnstein - Group III Condensed Matter ·Volume 41C: ``Non-Tetrahedrally Bonded Elements and Binary Compounds I'' in SpringerMaterials (https://doi.org/10.1007/10681727{_}62). https://doi.org/10.1007/10681727_62
[36] Malerba, C., Biccari, F., Ricardo, C.L.A., Valentini, M., Chierchia, R., Müller, M., Santoni, A., Esposito, E., Mangiapane, P., Scardi, P., Mittiga, A., 2014. CZTS stoichiometry effects on the band gap energy. J. Alloys Compd. 582, 528–534. https://doi.org/10.1016/j.jallcom.2013.07.199
[37] Rahman, I.A., Purqon, A., 2017. First Principles Study of Molybdenum Disulfide Electronic Structure, in: Journal of Physics: Conference Series. IOP Publishing, p. 012026. https://doi.org/10.1088/1742-6596/877/1/012026
[38] NREL, n.d. Reference Air Mass 1.5 Spectra | Grid Modernization | NREL (WWW Document). ASTM G-173-03. URL https://www.nrel.gov/grid/solar-resource/spectra-am1.5.html (accessed 9.1.21).